Optical Materials 167 (2025) 117249

Contents lists available at ScienceDirect

Optical Materials

journal homepage: www.elsevier.com/locate/optmat

Research article

Self-induced parabolic surface states

Damir V. Mitić [a], *, Jadranka M. Vasiljević [a], Dejan V. Timotijević [b], Dragana M. Jović Savić [a]

[a] Institute of Physics Belgrade, University of Belgrade, Pregrevica 118, 11080, Belgrade, Serbia

[b] Institute for Multidisciplinary Research, University of Belgrade, Kneza Višeslava 1, 11030, Belgrade, Serbia

ARTICLE INFO

MSC:
78-05
78A60

Keywords:
Surface states
Non-diffracting beam

ABSTRACT

We observed parabolic surface states during the nonlinear propagation of a Weber beams in an SBN crystal. The refractive index is modulated anisotropically using the optical induction technique. These states appear without the need for a pre-inscribed lattice in the material. Their characteristics can be tuned by adjusting the Weber beam's scale, parabolicity, orientation, and power. We also observed oscillatory discrete surface states during the linear propagation of a probe Gaussian beam within the aperiodic Weber photonic lattice. In both cases, such specific parabolic states are observed as surface states extending across multiple adjacent parabolas, or edge parabolic states localized along the border parabola. Our approach presents the first demonstration of self-induced parabolic surface states in aperiodic systems.

1. Introduction

Non-diffracting beams, exhibiting unique spatial structures and self-healing properties [1–4], have considerable interest in applications such as imaging, optical trapping, nonlinear and quantum optics [5–12]. Among them, Weber beams [13] form a class of non-diffracting optical waves with aperiodic transverse profiles in parabolic cylindrical coordinates. These beams can be generated using spatial light modulators that imprint the necessary phase structure onto an input wavefront [14]. Within their stability range, they offer significant promise for generating novel types of optical lattice [15,16], but their potential in nonlinear photonics remains still unexplored [17].

Electromagnetic waves located near the interface between two different media, known as surface modes, have attracted considerable attention due to their unique physical properties and potential applications in all-optical switching and sensing [10,18,19]. In optics, surface waves can arise at the interface between a continuous and a periodic medium and between different waveguide arrays [10]. Truncating photonic lattices leads to the formation of localized surface states, as demonstrated in 1D waveguide arrays [20] and 2D photonic lattices [21]. Surface state effects offer an additional mechanism for light confinement and expands the possibilities for controlling light with photonic lattices. The generation of lattice edges with various shapes remains an underexplored area with significant potential in nonlinear photonics [16].

In this paper, we extend the concept of surface state generation by investigating the nonlinear propagation of non-diffracting Weber beams in photorefractive media. Specifically, we observe the formation of *parabolic* surface states induced by refractive index modulation during the nonlinear propagation of Weber beams in photorefractive media. Unlike the surface states observed in truncated photonic lattices [18–21], our approach enables the observation of surface states *with no* permanent lattice structure inscribed in the material in advance. These states are generated through single-pass experiments and are supported by numerical simulations that closely match the experimental results. Such specific states are observed in the form of surface states that extend across multiple adjacent parabolas or edge parabolic states localized along the border parabola. We demonstrate precise control over the properties of the parabolic surface states by tuning the initial parameters of the Weber beam such as its scale, parabolicity, and orientation, as well as the degree of nonlinearity, governed by the beam power. Specifically, we can control the shape and parabolically of such surface states. Furthermore, we investigate the linear propagation of a narrow Gaussian probe beam in a Weber aperiodic lattice inscribed in photorefractive crystal (SBN61:Ce) to study surface effects. Under specific parameter regimes, we observe oscillatory surface states near the lattice boundary, characterized by cyclic energy exchange between adjacent lattice sites. They are observed as surface states extending across multiple adjacent parabolas, or edge parabolic states along the border parabola. These approaches enhance the predictability and control of the parabolic surface states, enabling new ways to manage diffraction, localization, topological states, and exploring novel nonlinear optical effects. These findings not only contribute to theoretical advances in

* Corresponding author.
E-mail address: damir@ipb.ac.rs (D.V. Mitić).

https://doi.org/10.1016/j.optmat.2025.117249
Received 27 May 2025; Received in revised form 10 June 2025; Accepted 16 June 2025
Available online 28 June 2025

optics and photonics but also pave the way for a range of practical applications such as optical information processing, communications, and biophotonics.

2. Numerical model for investigation of parabolic surface states

To investigate Weber beam propagation in strontium barium niobate (SBN61:Ce) crystal we use the nonlinear Schrödinger equation

$$i\partial_z A(r) + \frac{1}{2k_z}\left[\Delta_\perp + G(I)\right] A(r) = 0, \tag{1}$$

and spectral split step propagation method [22–24]. It relates to the paraxial propagation of the scalar light field A(r) with longitudinal wave vector k_z in a nonlinear potential $G(I) = -k_z^2 n_e^2 r_{33} E(I)$ defined by photorefractive nonlinearity, where $n_e = 2.35$ is the extraordinary bulk refractive index, $r_{33} = 267\,\mathrm{pm/V}$ is the corresponding electro-optical coefficients of the SBN61:Ce crystal and the wave number $k = 2\pi/\lambda = \sqrt{(k_\perp^2 + k_z^2)}$ is defined by the laser wavelength $\lambda = 532\,\mathrm{nm}$. The total electric field $E(I) = E_{\mathrm{ext}} + E_{\mathrm{sc}}(I)$ that builds up inside the crystal is a superposition of an external electric field $E_{\mathrm{ext}} = 2000\,\mathrm{V/cm}$ applied aligned with the optical $c = y$ axis (perpendicular to the propagation direction z-axis) to induce the photorefractive effect in the crystal and an internal electric space charge field E_{sc} that results from the incident intensity distribution $I = |A(r)|^2$ within the potential equation. We calculate the resulting intensity-depended, nonlocal, saturable, and anisotropic refractive index modulation [25] via $E_{sc} = \partial_x \phi_{sc}$ by numerically solving the anisotropic potential equation for the spatial evolution of the electrostatic potential ϕ_{sc} of the optically-induced space-charge field E_{sc}

$$\Delta_\perp \phi_{\mathrm{sc}} + \nabla_\perp \ln(1+I) \cdot \nabla_\perp \phi_{\mathrm{sc}} = E_{\mathrm{ext}} \partial_x \ln(1+I), \tag{2}$$

as shown in previous works of us [23,24] where I is obtained from Eq. (1). Subsequently, Eq. (1) is updated with the optically induced space-charge field $E_{sc} = \partial_x \phi_{sc}$, obtained by solving Eq. (2). This procedure is iteratively repeated along the propagation direction z.

Anisotropic model, consisting of Eqs. (1) and (2), is appropriate for investigation of Weber beam propagation in the SBN61:Ce crystal because this crystal is inherently anisotropic. While saturation reduces effective nonlinearity at high intensities, limiting the maximum achievable index change and affecting the confinement and existence of surface states, nonlocality introduces spatial averaging, which enhances stability, but may broaden or shift surface-bound modes, reducing their localization. Together, saturation and nonlocality critically determine the shape, stability, and threshold conditions of surface states and guided modes in SBN61:Ce.

As the paraxial scalar light field A (structure beam in the experiment), we use even Weber beams [13]

$$A = U_e(\eta, \xi; a) = \frac{1}{\pi\sqrt{2}} |\Gamma_1|^2 P_e(\sigma\xi; a) P_e(\sigma\eta; -a), \tag{3}$$

where P_e is even parabolic cylinder function, Γ is Gamma functions, $\Gamma_1 = \Gamma[(1/4) + (1/2)ia]$, $\sigma = (4\pi/\lambda)^{1/2}$, ($\xi$, η) are parabolic cylinder coordinates, and the parameter a determines the curvature of the Weber beam lobes and acts as an indicator of parabolicity. The relationship between parabolic cylinder coordinates (ξ, η) and spatial Cartesian coordinates (x, y) is defined by coordinate transformations $\xi = \sqrt{x + \sqrt{x^2 + y^2}}$ and $\eta = \sqrt{\sqrt{x^2 + y^2} - x}$. Odd beams yield similar results.

3. Experimental method for parabolic surface states generation

The experimental optical induction technique is used that allows refractive index changes of the photorefractive material, a birefringent cerium-doped strontium barium niobate crystal (SBN61:Ce). The experimental setup is shown in Fig. 1. As a light source, we use a continuous frequency-doubled Nd:YVO_4 laser with a wavelength of $\lambda = 532\,\mathrm{nm}$. The

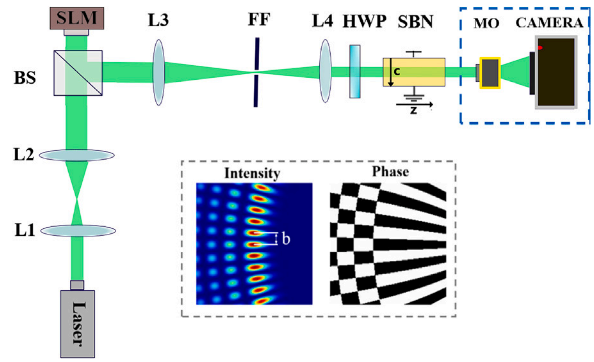

Fig. 1. Experimental setup for investigating the nonlinear propagation of Weber beams. L — lens, BS — depolarized beam splitter, SLM — spatial light modulator, FF — Fourier filter, SBN — medium, HWP — half-wave plate, MO — 10x microscope objective. Inset presents one example of Weber beam intensity and phase distributions, with typical beam scale indicated with b.

linearly polarized laser beam is spatially modulated using a phase-only full HD HOLOEYE PLUTO-2.1 LCoS SLM, with resolution 1920 × 1080, featuring a pixel pitch of 8 μm, to generate the desired beam structure, inducing a corresponding refractive index modulation in the biased photosensitive crystals. Although inherently phase-only, the SLM enables simultaneous modulation of both the amplitude and phase of the reflected light field by displaying a precomputed hologram of a Weber beam superimposed with an additional blaze grating and Fourier filtering in the Fourier plane of lens L3 [14]. Then, a spatially modulated initiation laser beam from SLM passes through several optical elements, including lenses, a beamsplitter, and a pinhole, before it illuminates the crystal. The SBN61:Ce crystal, with dimensions of $5 \times 5 \times 20\,\mathrm{mm}^3$, is biased to an external electric field (E_{ext}), applied along the optical $c = y$ axis. This electric field is perpendicular to the wave propagation direction (the z-axis). As a result, the extraordinarily polarized structure light field with power (P_w) propagates through the crystal. Changing beam power P_w affects different nonlinearity strengths. The SBN61:Ce crystal provides strong nonlinearity at comparatively low power levels. We used powers that are reproducible for our results. Such powers are below the threshold for optical damage. This crystal is doped with cerium (Ce), a dopant known to improve resistance to optical damage. We used an imaging system with a 10x microscope objective (MO) and camera to observe the transverse intensity distribution on the exit face of the crystal.

Typical examples of parabolic surface states induced by nonlinear self-action are shown in Fig. 2. Parabolic surface states can be localized on few adjacent parabolas (Fig. 2(a)). Another representative example is the edge surface state, localized along the edge parabola (Fig. 2(b)). The characteristics of these states can be effectively controlled by adjusting the Weber beam's parabolicity, scale, and intensity (power).

4. Self-induced parabolic surface states obtained during the nonlinear propagation of Weber beams

We begin our investigation with Weber beams with varying parabolicities, scales, and orientations to study how their propagation behavior changes with increasing beam power. At low beam powers, the beams propagate stable along the length of the crystal, maintaining their symmetry and non-diffracting nature. As the power increases, stability is broken, and the beams lose their non-diffracting characteristics. At these lower powers, parabolic surface states extending across multiple adjacent parabolas are observed. With further increases in power, surface states become localized along the border parabola, so we call them parabolic edge states. At the highest beam powers, we observe the migration of parabolic surface states along an adjacent parabola,

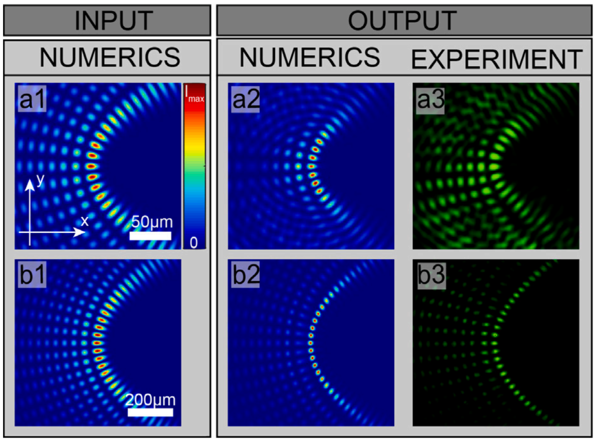

Fig. 2. Representative examples of self-induced parabolic surface states. First column: Intensity distributions of Weber beams at the input. The second and third columns: Intensity distributions at the exit face of the crystal obtained numerically (the second column) and experimentally (the third column), after 20 mm propagation distance. Parameters are: (a) $a = 6$, $b = 12$ μm, $I = 0.7$, $P_w = (34 \pm 1.02)$ μW and (b) $a = 10$, $b = 35$ μm, $I = 0.08$, $P_w = (3.4 \pm 0.102)$ μW.

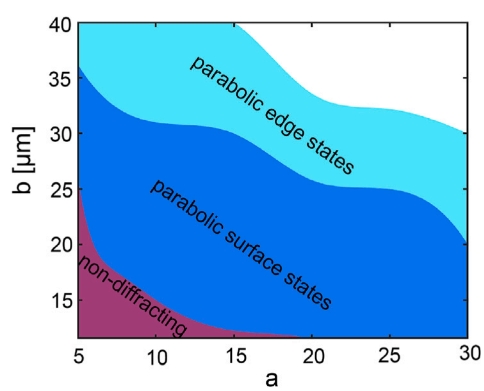

Fig. 3. (a) Parameter space diagram with different regimes of the Weber beam propagation in nonlinear regime. b is Weber beam scale, and a is parabolicity of Weber beam. Input beam intensity $I = 0.16$ [$a.u.$].

indicating a dynamic transitions and modulation instabilities. Quantitative thresholds for transition between two regions depend on the Weber beam parameters such as beam scale, parabolicity, and orientation. Threshold values for intensity/power corresponding to transitions between regions can be defined only for one fixed set of these three parameters.

Fig. 3 provides a detailed phase diagram of the Weber beam scale b and parabolicity a, for the Weber beam intensity $I = 0.16$. At lower values of either or both parameters, the Weber beams remain stable during propagation, preserving their non-diffracting character. As these parameters are increased, there is a region of parabolic surface states across a few adjacent parabolas, but further increasing both parameters leads to the formation of parabolic edge states. At the highest values of the control parameters, modulation instabilities can be observed (white region in parameter space). By adjusting the beam's parameters, the shape and parabolicity of the surface state can be precisely controlled and fine-tuned.

Fig. 4 illustrates the effect of the Weber beam scale parameter b on the formation of parabolic surface states. At lower values of b, the beam structure remains almost stable, with only minimal energy transfer to neighboring parabolas. As b increases, a variety of two-dimensional surface states emerge. These results demonstrate that tuning the scale

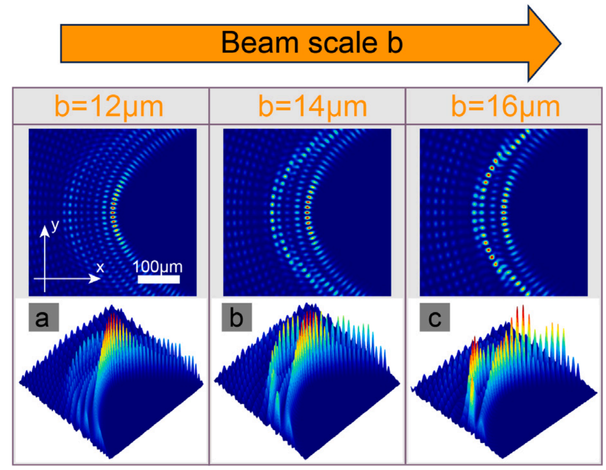

Fig. 4. Influence of Weber beam scale on the formation of the parabolic surface states. Transverse intensity distributions of Weber beam after 20 mm propagation. Parameters: Weber beam parabolicity $a = 15$, and input intensity $I = 0.3$.

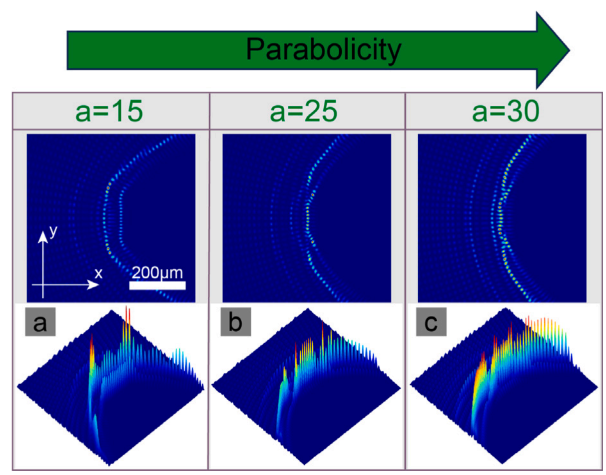

Fig. 5. Influence of Weber beam parabolicities on the formation of the parabolic surface states. Transverse intensity distributions of Weber beam after 20 mm propagation. Parameters: Weber beam structure size $b = 15$ μm, and input intensity $I = 0.8$.

parameter b allows precise control over the shape and curvature of the surface states, enabling fine adjustments to their spatial structure.

The influence of Weber beam parabolicity a on the formation of parabolic surface states at high beam intensities I, corresponding to increased power in the experiment, is presented in Fig. 5. Under these conditions, various surface state configurations emerge, predominantly localized near the border and adjacent parabola. By varying the parabolicity of the beam, it becomes possible to independently control the curvature, shape, and spatial extent of self-induced surface states, offering a high degree of surface states tunability.

5. Oscillatory surface states obtained during linear propagation of Gaussian probe beam in Weber lattice

At the end, we investigate the effects during the *linear* propagation of a narrow Gaussian probe beam near the edge of various aperiodic Weber photonic lattices. Weber photonic lattices are naturally truncated, therefore build-up processes such as multiplexing or some kind of occlusion is avoided for their generation. First, we find parameters for the generation of photonic lattices using Weber beams of various parabolicity, scale, and orientation. The process of photonic lattice generation is modeled through the potential $I = I_{latt}$ in Eq. (1). We

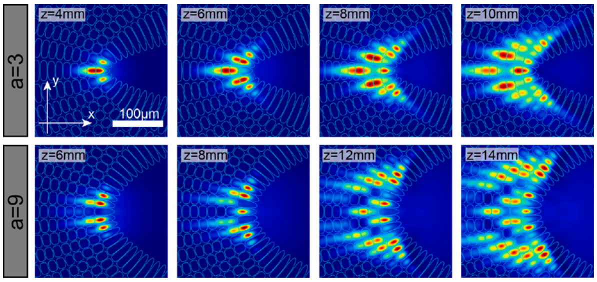

Fig. 6. Discrete surface states. Transverse intensity distributions of probe Gaussian beam in aperiodic Weber lattice with parabolicity: $a = 3$ (the first row), $a = 9$ (the second row), at various propagation distances, marked at individual figures. Contours indicate Weber lattice position. Parameters: $b = 12$ μm, and lattice intensity $I_{latt} = 0.5$.

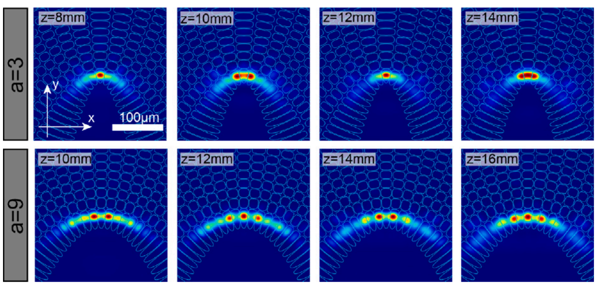

Fig. 7. Discrete edge states. Transverse intensity distributions of probe Gaussian beam in aperiodic Weber lattice with parabolicity: $a = 3$ (the first row) and $a = 9$ (the second row), at various propagation distances, marked at individual figures. Contours indicate Weber lattice position. Parameters: $b = 12$ μm, and lattice intensity $I_{latt} = 0.5$.

obtain the spatial distribution of I_{latt} through a separate numerical simulation of Eqs. (1) and (2) based on propagation of an ordinary Weber beam under weak nonlinearity, finding the fixed value of I_{latt} for the formation of the uniform lattice along the propagation distance. Then, we use such an obtained distribution as the lattice potential for the simulation of extraordinary Gaussian probe beam propagation using equations modified such that $I = I_p + I_{latt}$, where the Gaussian probe beam intensity $I_p = |A|^2$ is obtained from Eq. (1). Gaussian probe beam width is sufficient to cover one lattice site. In our probing simulations I_p is sufficiently weak so as not to cause nonlinear modification [12].

We study how the variation in the parabolicity of the Weber lattice a influences the discrete diffraction of light and the formation of surface states. Furthermore, we consider two different orientations of the Weber lattice, as presented in Figs. 6 and 7. We perform our investigation by probing Weber lattices with various parabolicities $a = 3$ and $a = 9$. The input position of the probe beam is at the central lattice site along the edge (outer) parabola. In all figures, the white contours overlaid on the intensity distributions indicate the positions of the waveguides.

For the lattice orientation shown in Fig. 6, we observe oscillatory discrete surface states. With increasing propagation distance, the probe beam gradually spreads from the edge towards the inner lattice sites. In contrast, the lattice orientation presented in Fig. 7 supports edge surface states that remain confined to the lattice edge. This difference is attributed to the anisotropic properties of the photorefractive crystal. In both lattice orientations, oscillatory surface effects are evident, characterized by an alternating excitation of the central site and its two nearest neighbors.

Surface states observed with linear probe beam propagation in the Weber lattice could provide predictions and appropriate parameters for nonlinear self-induced surface states. The anisotropy of the SBN crystal is an additional control factor, allowing various surface states to be obtained along a different orientation. For both linear and nonlinear surface states, we have fine-tuning for various surface states covering a few parabolas or only the one (border) parabola.

6. Conclusion

We have developed a method for generation of parabolic surface states in photorefractive media using a single-pass experimental setup and optical induction. Our results demonstrate that nonlinear Weber beams can induce parabolic surface states without the need for prefabricated lattices or lattice truncation. We systematically investigated how these surface states depend on the strength of the nonlinearity, as well as on the scale, parabolicity, and orientation of the Weber beam. This approach enables precise control over the shape and curvature of the parabolic surface states, offering new opportunities to design beam structures with complex topologies and manage novel surface phenomena. Also, we have shown parabolic discrete oscillatory surface states during the linear propagation of Gaussian probe beam in aperiodic Weber photonic lattice. These findings not only advance the theoretical understanding of light–matter interactions in nonlinear photonics but also open new possibilities for applications in optical information processing, communication technologies, and biophotonics.

CRediT authorship contribution statement

Damir V. Mitić: Visualization, Methodology, Investigation. **Jadranka M. Vasiljević:** Investigation, Data curation. **Dejan V. Timotijević:** Writing – review & editing, Software, Conceptualization. **Dragana M. Jović Savić:** Writing – original draft, Supervision.

Declaration of competing interest

The authors declare the following financial interests/personal relationships which may be considered as potential competing interests: Dragana Jović Savić, Dejan Timotijević and Jadranka Vasiljević reports financial support was provided by Fund of the Republic of Serbia, GRANT No 7714356, IDEAS - CompsLight. If there are other authors, they declare that they have no known competing financial interests or personal relationships that could have appeared to influence the work reported in this paper.

Acknowledgments

The authors acknowledge funding provided by the Institute of Physics Belgrade and Institute for Multidisciplinary Research (IMSI), through the grants by the Ministry of Science, Technological Development and Innovations of the Republic of Serbia (IMSI contract no. 451-03-66/2024-03/200053) and by the Science Fund of the Republic of Serbia, GRANT No 7714356, IDEAS - CompsLight.

Data availability

Data will be made available on request.

References

[1] J. Durnin, Exact solutions for nondiffracting beams. I. The scalar theory, J. Opt. Soc. Amer. A 4 (1987) 651–654.
[2] J. Durnin, J.J. Miceli, J.H. Eberly, Diffraction-free beams, Phys. Rev. Lett. 58 (1987) 1499–1501.
[3] E.G. Kalnins, J. W. Miller, Lie theory and separation of variables. 9. Orthogonal R-separable coordinate systems for the wave equation $\Psi_{tt} - \Delta_2\ \Psi = 0$, J. Math. Phys. 17 (1976) 331–355.
[4] J.C. Gutiérrez-Vega, M.D. Iturbe-Castillo, S. Chávez-Cerda, Alternative formulation for invariant optical fields: Mathieu beams, Opt. Lett. 25 (2000) 1493–1495.
[5] M. Woerdemann, C. Alpmann, M. Esseling, C. Denz, Advanced optical trapping by complex beam shaping, Laser Photon. Rev. 7 (2013) 839–854.

[6] V. Garcés-Chávez, D. McGloin, H. Melville, W. Sibbett, K. Dholakia, Simultaneous micromanipulation in multiple planes using a self-reconstructing light beam, Nature 419 (2022) 145–147.

[7] J. Baumgartl, M. Mazilu, K. Dholakia, Optically mediated particle clearing using airy wavepackets, Nat. Photonics 2 (2008) 675–678.

[8] J.W. Fleischer, M. Segev, N.K. Efremidis, D.N. Christodoulides, Observation of two-dimensional discrete solitons in optically induced nonlinear photonic lattices, Nature 422 (2003) 147–150.

[9] H. Martin, E.D. Eugenieva, Z. Chen, D.N. Christodoulides, Discrete solitons and soliton-induced dislocations in partially coherent photonic lattices, Phys. Rev. Lett. 92 (2004) 123902.

[10] F. Lederer, G.I. Stegeman, D. Christodoulides, G. Assanto, M. Segev, Y. Silberberg, Discrete solitons in optics, Phys. Rep. 463 (2008) 1–126.

[11] J.M. Vasiljević, A. Zannotti, D.V. Timotijević, C. Denz, D.M.J. Savić, Light transport and localization in disordered aperiodic Mathieu lattices, Opt. Lett. 47 (3) (2022) 702–705.

[12] J.M. Vasiljević, V.P. Jovanović, A.Ž. Tomović, D.V. Timotijević, R. Žikic, M.R. Belić, D.M.J. Savić, Interdimensional radial discrete diffraction in mathieu photonic lattices, Opt. Express 31 (18) (2023) 28946–28953.

[13] M.A. Bandres, J.C. Gutiérrez-Vega, S. Chávez-Cerda, Parabolic nondiffracting optical wave fields, Opt. Lett. 29 (2004) 44–46.

[14] J.A. Davis, D.M. Cottrell, J. Campos, M.J. Yzuel, I. Moreno, Encoding amplitude information onto phase-only filters, Appl. Opt. 38 (1999) 5004–5013.

[15] P. Rose, M. Boguslawski, C. Denz, Nonlinear lattice structures based on families of complex nondiffracting beams, New J. Phys. 14 (2012) 033018.

[16] A.Ž. Tomović, I.J.V. Mitić, V.P. Jovanović, D.V. Timotijević, D.M.J. Savić, Assembling of truncated deterministic aperiodic lattices with defects using Weber beams, Opt. Mater. 157 (2024) 116334.

[17] B. Freedman, G. Bartal, M. Segev, R. Lifshitz, D.N. Christodoulides, J. Fleisher, Wave and defect dynamics in nonlinear photonic quasicrystals, Nature 440 (2006) 1166–1169.

[18] S. Suntsov, K.G. Makris, G.A. Siviloglou, R. Iwanovw, R. Schiek, D.N. Christodoulides, G.I. Stegeman, R. Morandotti, H. Yang, G. Salamo, M. Volatier, V. Aimez, R. Arès, M. Sorel, Y. Min, W. Sohler, X. Wang, A. Bezryadina, Z. Chen, Observation of one and two-dimensional discrete surface spatial solitons, J. Nonlinear Opt. Phys. Mater. 16 (04) (2007) 401–426.

[19] Y.S. Kivshar, Nonlinear tamm states and surface effects in periodic photonic structures, Laser Phys. Lett. 5 (10) (2008) 703.

[20] C.R. Rosberg, D.N. Neshev, W. Krolikowski, A. Mitchell, R.A. Vicencio, M.I. Molina, Y.S. Kivshar, Observation of surface gap solitons in semi-infinite waveguide arrays, Phys. Rev. Lett. 97 (2006) 083901.

[21] X. Wang, A. Bezryadina, Z. Chen, K.G. Makris, D.N. Christodoulides, G.I. Stegeman, Observation of two-dimensional surface solitons, Phys. Rev. Lett. 98 (2007) 123903.

[22] G. Agrawal, Nonlinear Fiber Optics, fifth ed., Academic Press, 2012.

[23] A. Zannotti, J.M. Vasiljević, D.V. Timotijević, D.M.J. Savić, C. Denz, Morphing discrete diffraction in nonlinear mathieu lattices, Opt. Lett. 44 (7) (2019) 1592–1595.

[24] A. Zannotti, J.M. Vasiljević, D.V. Timotijević, D.M. Jović Savić, C. Denz, Visualizing the energy flow of tailored light, Adv. Opt. Mater. 6 (8) (2018) 1701355.

[25] A.A. Zozulya, D.Z. Anderson, Propagation of an optical beam in a photorefractive medium in the presence of a photogalvanic nonlinearity or an externally applied electric field, Phys. Rev. A 51 (1995) 1520–1531.

Book of abstracts

PHOTONICA 2025

X International School and Conference on Photonics

25 - 29 August 2025

Belgrade, Serbia

Editors

Mihailo Rabasović, Uroš Ralević, Marina Lekić, Aleksandar Krmpot
Institute of Physics Belgrade, Serbia

Belgrade, 2025

Excitation of self-induced surface states in parabolic geometry

D. V. Mitić[1], J. M. Vasiljević[1], D. V. Timotijević[2], and D. M. Jović Savić[1]
[1]*Institute of Physics, University of Belgrade, P.O. Box 68, 11001 Belgrade, Serbia*
[2]*Institute for Multidisciplinary Research, University of Belgrade, Kneza Višeslava 1, 11030, Belgrade, Serbia*
e-mail: damir@ipb.ac.rs

Non-diffracting beams are a class of optical waves that maintain their transverse intensity profile over long propagation distances, exhibiting self-healing properties [1-5]. These beams have found applications in the field of optical trapping, high-resolution imaging, and laser material processing, where precise beam control and long-depth focusing are essential [6]. They are a significant promise for a new class of optical lattice-writing light within their stability range [7], but their potential in nonlinear photonics remains unexplored [8]. Truncating photonic lattices leads to the formation of localized surface states demonstrated in 1D waveguide arrays and 2D photonic lattices [9]. The geometrical characteristics of Weber beams offer a specific level of control over the topology of lattice surface.

We achieve the progress of these fields extending the concept of surface state generation by investigating the nonlinear propagation of non-diffracting Weber beams in photorefractive media. We present an approach for generating self-induced parabolic surface states in a photorefractive SBN crystal, utilizing a single-pass experimental setup with the optical induction technique. We systematically examined how these surface states characteristics depend on the beam parameters, orientation, and the strength of the nonlinearity. The formation of these surface states was observed without a pre-inscribed photonic lattice. This approach enhances the predictability and control of parabolic surface states, enabling new ways to manage diffraction, localization, and exploring novel nonlinear optical effects. Also, we investigate the linear propagation of a narrow Gaussian probe beam in a Weber aperiodic lattice inscribed in an SBN crystal to study surface effects. Such photonic lattices are naturally truncated, therefore build-up processes such as multiplexing or some kind of occlusion is avoided for their generation. Under specific parameter regimes, we observe oscillatory surface states near the lattice boundary, characterized by cyclic energy exchange between adjacent lattice sites. In both cases, such specific parabolic states are observed in the form of surface states extending across multiple adjacent parabolas, or edge parabolic states localized along the border parabola.

REFERENCES

[1] J. Durnin, J. Opt. Soc. Am. A 4, 651 (1987).
[2] J. Durnin, J. J. Miceli, and J. H. Eberly, Phys. Rev. Lett. 58, 1499 (1987).
[3] E. G. Kalnins and J. W. Miller, J. Math. Phys. 17, 331 (1976).
[4] J. C. Gutiérrez-Vega, M. D. Iturbe-Castillo, and S. Chávez-Cerda, Opt. Lett. 25, 1493 (2000).
[5] M. A. Bandres, J. C. Gutiérrez-Vega, and S. Chávez-Cerda, Opt. Lett. 29, 44 (2004).
[6] M. Woerdemann, C. Alpmann, M. Esseling, and C. Denz, Laser Photon. Rev. 7, 839 (2013).
[7] P. Rose, M. Boguslawski, and C. Denz, New Journal of Physics14, 033018 (2012).
[8] B. Freedman, G. Bartal, M. Segev, R. Lifshitz, D. N. Christodoulides, and J. Fleisher, Nature 440, 1166 (2006).
[9] S. Suntsov, at. al, Journal of Nonlinear Optical Physics & Materials 16, 401 (2007).
[10] D.V. Mitić, J. M. Vasiljević, D. V. Timotijević, and D. M. Jović Savić, *Self-induced parabolic surface states* Submitted in Optical Materials.

ORCID: D.M. 0009-0003-0085-9448, J.V. 0000-0001-9092-5223, D.T. 0000-0003-4538-3140, D.J.S, 0000-0002-1081-0141